

Designing polymer blends for extreme environments: from low earth orbits to nanocomposites

Nilay K. Roy^{1,2,*}

¹ITS - Research Computing, Northeastern University, 360 Huntington Avenue, Boston, MA 02115, USA.

²Current affiliation: The Charles Stark Draper Laboratory, Inc. (Draper), 555 Technology Square, Cambridge, MA 02139-3563, USA.

ABSTRACT

The production of materials with end-use properties, and high performance materials in low temperature environments, or where radiation is high, is difficult. Low earth orbit is one place where in addition to micro level space debris and extremes in temperatures, the requirement is for long-lasting materials with no degradation from these effects. On the nanolevel the challenges of developing new composites using nanotubes and exfoliated graphite scaffolds also need computational methods to be used in the design. The design of new materials using polymer blending methods speeds up and is enhanced by high performance computing simulations, that also predict the behavior of these materials. This paper covers current computational methods in designing polymer blends for extreme environments, and simulation strategies to predict the behavior in such environments.

KEYWORDS: polymer blends, miscibility, nanocomposites, high-performance materials, scaffolds, extreme environments, low earth orbits, permeation path, ionomeric membrane, sequence-controlled polymers.

1. Introduction

Polymer blend miscibility is an exception not a rule. To get a useful material that incorporates the

best properties of the parent requires, in high molecular weight polymer systems, miscibility. Various techniques exist that can at the thermodynamic level enable miscibility. These include using compatibilizers and plasticizers and anti-plasticizers among others. Copolymerization with blending using a backbone like nanotubes is also used with multiphase copolymers. Designing a new mer and polymerizing it is rarely attempted. The new material from the blend design, like thermoplastic elastomers, forms the majority of plastics used today – e.g. ABS plastics. While these have a range of uses, are easy to produce and provide the core in all material use, they lack things like biodegradability, flame retardancy, and stability in extreme environments like space, on the nanoscale, and in the human body. Bench work to design new materials and introduce the new properties and capabilities into existing materials is beyond the scope of any manufacturer. The only way to achieve reasonable success is to use computational/simulation methods like that described in [1-2]. Large-scale computations rapidly narrow down the alternatives and provide thermodynamic insight to methods for achieving miscibility, and thus new materials with targeted end-use properties. It is now possible to design materials with targeted end-use properties, performance and failure ratings with minimal experimentation as well as incorporate several alternatives to test in the lab the quickest way to eventually manufacture such a material.

*Email id: nroy@draper.com

2. Current techniques

Processes on different length scales affect the dynamic properties of polymer melts and blends. However these dynamics are studied in blends that are miscible on a thermodynamic scale [3-8]. Some important examples of predicting miscibility include equation of state approaches for pure polymer fluids, solutions, and blends [9-11]. In many instances polymer blends are partially miscible demonstrating upper critical solution temperature (UCST)-type or lower critical solution temperature (LCST)-type immiscibility or phase separation. The former exhibit phase separation only upon lowering of temperature (yielding an upper critical solution temperature, or UCST). In the latter immiscibility occurs upon an increase in temperature (yielding a lower critical solution temperature, or LCST). It has become apparent that many experimental examples of partially miscible blends of both

UCST and LCST-type can be found (Figure 1). A widely used model is based on equation of state-type descriptions – the lattice-fluid model. It models polymeric melts and blends. The theory accounts for both the effects of compressibility and nonrandom mixing, thereby moving several steps beyond Flory-Huggins theory [12]. The derivations [13] follow an integral equation formalism in which site-site (pair) probabilities are calculated for all possible neighboring pairs of segments in the chain fluid. These temperature-dependent probabilities are used to calculate the system's internal energy, which can be integrated over temperature (starting from an athermal reference state) to give a closed-form expression for the Helmholtz free energy (A), thereby leading to all of the other thermodynamic quantities.

The analytic result for A is shown in Eq. 1 for the case of a binary mixture comprised of components i and j

$$\begin{aligned} \frac{A}{k_B T} = & N_i \ln \phi_i + N_j \ln \phi_j + N_h \ln \phi_h + \frac{N_i q_i z}{2} \ln(\xi_i / \phi_i) + \frac{N_j q_j z}{2} \ln(\xi_j / \phi_j) + \frac{N_h z}{2} \ln(\xi_h / \phi_h) - \\ & \frac{N_i q_i z}{2} \ln[\xi_i \exp(-\epsilon_{ii} / k_B T) + \xi_j \exp(-\epsilon_{ij} / k_B T) + \xi_h] - \frac{N_j q_j z}{2} \ln[\xi_i \exp(-\epsilon_{ij} / k_B T) + \xi_j \exp(-\epsilon_{jj} / k_B T) + \xi_h] \end{aligned} \quad (1)$$

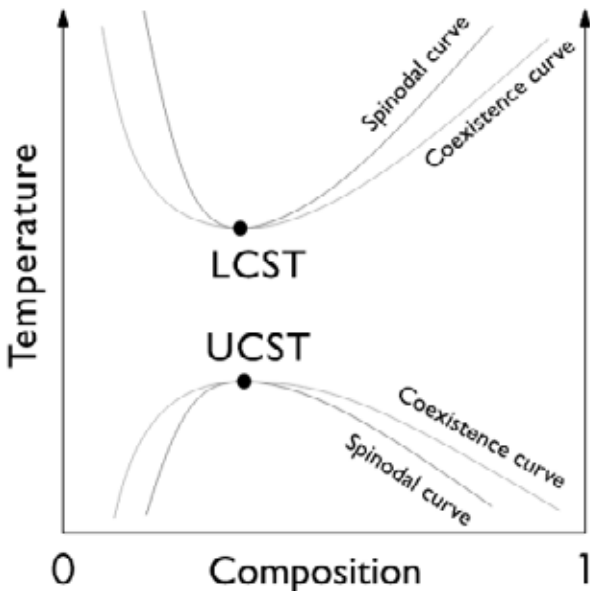


Figure 1. A plot of typical polymer binary solution phase behavior including both an LCST and a UCST.

with definitions

$$N_h = \left(\frac{V}{v} \right) - N_i r_i - N_j r_j$$

$$\phi_\alpha = N_\alpha r_\alpha v / V$$

$$\xi_\alpha = N_\alpha q_\alpha / (N_i r_i + N_j r_j + N_h)$$

$$q_\alpha z = r_\alpha z - 2r_\alpha + 2$$

where α can be i, j , or h , and $q_h = r_h = 1$. In Eq. 1, A is expressed as a function of independent variables N_i, N_j, V , and T which are the numbers of molecules of components i and j , the total volume, and the absolute temperature, respectively. z is the lattice coordination number which is fixed at a value of 6, and k_B is the Boltzmann constant. The key microscopic lattice parameters are v , the volume per lattice site, r_i (r_j), the number of segments per chain molecule of component i (j), ϵ_{ii} (ϵ_{ij}), the pure

component nonbonded segment–segment interaction energy between near-neighbor segments of types i – i (j – j), and g , which defines the mixed interaction energy according to $\varepsilon_{ij} = g(\varepsilon_{ii}\varepsilon_{jj})^{1/2}$ (g characterizes ε_{ij} relative to the geometric mean value). The model is compressible, so the total volume, V , is comprised of filled and empty lattice sites. Therefore, N_h is the total number of vacant sites (h stands for “holes”); this value increases with V for any given N_i , N_j . The remaining definitions in Eq. 1 are as follows: ϕ_α is the volume fraction of sites of type α ($\alpha \in \{i, j, h\}$), and ζ_α is a concentration variable defining the fraction of nonbonded contacts ascribed to component α out of the total number of nonbonded contacts in the fluid, where, due to its bonded connections, a chain molecule has $q_\alpha z$ nonbonded contacts. Eq. 1 by differentiation leads to all other thermodynamic properties including pressure, Gibbs free energy, and the chemical potentials. While the pressure P is expressed as a function of V , V cannot be directly expressed as a function of P , and thus numerical root finding is commonly used to obtain V and other properties for cases where P is the known (input) variable. Sometimes it is more convenient to work with intensive variables giving three independent variables.

Now the blend modeling involves using conditions of phase equilibrium, and phase boundaries with the spinodal marking the metastability limit. Ref. [1] gives full details of working with dimensional parameters and obtaining the phase diagrams with respective compositions in each phase and the related critical points (temperature, composition and volume).

Several methods can be used to obtain the solutions. In [1] a new technique is described. However one can use other methods including fitting protocols. Once the miscibility regime is obtained dynamics can be studied. One method to model and study miscible system dynamics uses monomeric friction coefficients, which are inversely proportional to the mobility of short-chain segments. They are a convenient way to describe the effect of local dynamic properties on global dynamic properties such as the viscosity [14]. Since blending changes the local environment of the chain segments of a polymer it has a strong effect on the local dynamics of the chains. From experimental [15] and simulation works [16] it is found that the local dynamics of the two blend components differ from each other

and the pure melts. The addition of slow (high friction coefficient) component to a blend is found to increase the friction coefficients of both components and, conversely, the addition of fast component is found to speed up both components. The effects of blending are most pronounced near the glass transition; however, they are observed even at high temperatures [17] and in blends where one of the components is dilute [18]. Several recently developed models for miscible polymer blends relate differences in the component dynamics to local variations in the glass transition temperature induced by local variations in blend composition [19] while others consider “intrinsic” effects, due to differences in the chain structure of the two components, in addition to local density and composition variations [20–22]. Self-diffusion coefficients give information about the chain dynamics of polymer melts and blends. The Rouse model prediction for the self-diffusion coefficient of a polymer chain may be written as

$$D_r = \frac{k_B T}{\xi N} = \mu / N, \quad (2)$$

where T is the temperature, k_B is Boltzmann’s constant, N is the chain length, ζ is the so-called monomeric friction coefficient, and $\mu = k_B T / \zeta$ is the corresponding mobility. The long-time dynamics of long polymer chains are dominated by entanglement effects, which are not part of the Rouse model. The reptation model [23] describes the entanglements of a chain with other chains in terms of a tube, which restricts the motion of the chain perpendicular to the tube. In experimental work the entanglement length is often defined through its relation to the plateau modulus [24]. The characteristic chain length N_c that separates short-chain (unentangled) behavior from long-chain (entangled) behavior for viscoelastic properties is found to be related to this entanglement length by a constant factor [25]. Experimental, theoretical, and simulation works on polymer melts suggest that the tube diameter of the reptation theories is proportional to the packing length. The transition between the unentangled and entangled regimes is not sharp and simulation data are often found to be in the crossover region between unentangled and reptation behaviors [26].

It is convenient to rescale the chain length N by the characteristic chain length N_c $\propto N_e$ and the self-diffusion coefficient D by a characteristic

diffusion coefficient D_c . In this way, the predictions for the self-diffusion coefficient may be summarized as

$$\frac{D}{D_c} \propto \begin{cases} \left(\frac{N}{N_c}\right)^{-1} & \text{for } N \ll N_c \\ \left(\frac{N}{N_c}\right)^{-2} & \text{for } N \gg N_c \end{cases} \quad (3)$$

so that, at the chain length N_c , the extrapolations from both power laws yield the same value, $D/D_c=1$.

Simulation work on polymer blends has been carried out with atomistic and coarse grained models [27]. Molecular dynamics simulations of atomistic models give access to the chain structure and dynamics of realistic polymers and allow a detailed investigation of the environments of the chain segments [28]. Simulations of coarse-grained models, on the other hand, can be used to isolate particular effects such as isotope effects and differences in chain stiffness [29].

For Monte-Carlo Simulations Shaffer's bond fluctuation model is used [30]. It is a lattice model for polymer chains, where the monomers occupy sites of a simple cubic lattice. If the size of the unit cell, i.e., the lattice constant a , is the unit for length the monomers are connected by bonds of three possible lengths: 1, $\sqrt{2}$, and $\sqrt{3}$, corresponding to the sides, face diagonals, and body diagonals of the unit cell of the lattice. Monte Carlo simulations of the model employ only local moves, where an attempt is made to displace a randomly chosen monomer by one lattice site along any of the three coordinate directions. One attempted elementary move per monomer in the system is called one Monte Carlo step (MCS) and is the unit of time. Shaffer considered two versions of this model. In the first version, bonds are allowed to cross each other with the result that the chains do not entangle; in the second, bond crossings are prohibited and entanglement effects become apparent (Figure 2).

Another commonly used method involves large-scale molecular dynamics (MD) simulations [31]. Using force fields like the Dreiding force field [32], a two-step structural optimization process (energy evaluations and conformation adjustment) is done *via* standard NVT or NPT canonical ensemble MD. The coordinates of a structure combined with a force field create an energy expression (or a target function). This energy expression is the equation that describes the potential energy of a particular structure as a function of its atomic coordinates.

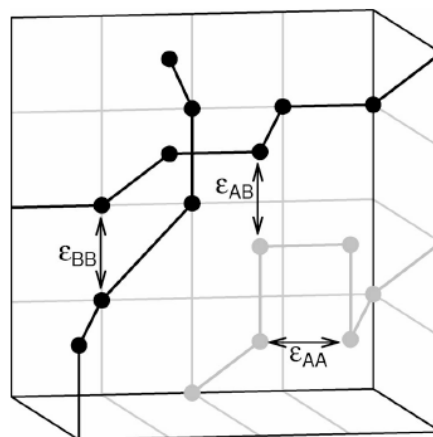


Figure 2. Illustration of the generalization of Shaffer's bond fluctuation model to polymer blends. The circles connected by heavy lines represent polymer chains in a blend, gray for component A and black for component B. Allowed bond lengths are 1, $\sqrt{2}$, and $\sqrt{3}$ corresponding to the sides, face diagonals, and body diagonals of the unit cell of the simple cubic lattice. The arrows show examples of nearest neighbor interactions between like (ϵ_{AA} and ϵ_{BB}) and unlike (ϵ_{AB}) monomers.

The total potential energy (E_{pot}) of the system is expressed as $E_{pot} = E_{valence} + E_{Crossterm} + E_{non-bond}$. The energy of valence interaction ($E_{valence}$) includes the stretching energy of the bond (E_{bond}), the bending energy of the valence angle (E_{angle}), the torsion energy of the dihedral angle ($E_{torsion}$) and the inversion energy called out-of-plane interaction (oop), which are part of nearly all forcefields for covalent systems. Cross-term energy ($E_{crossterm}$) has been used to account for such factors as bond or angle distortions caused by nearby atoms. These terms are necessary to reproduce with precision the vibrational frequencies and therefore, the dynamic properties of molecules. Finally, the energy of interactions between non-bonded atoms ($E_{non-bond}$) includes the van der Waals energy (E_{vdw}), hydrogen bond energy (E_{H-bond}) and Coulomb electrostatic energy ($E_{Coulomb}$). The conformation is adjusted to reduce the value of the energy expression. A minimum may be found after one adjustment or may require several thousand of iteration, depending on the nature of the algorithm, the form of the energy expression and the size of the structure. The efficiency of optimization is therefore judged both by the time required to evaluate the expression of energy and the number of structure adjustment (iterations) necessary to converge to a minimum. A modified Flory-Huggins

model and a molecular simulation technique [33] to calculate compatibility of polymer-polymer mixtures with two important extensions of the Flory-Huggins model are used: (i) An explicit temperature dependence on the interaction parameter. This is accomplished by generating a large number of pair configurations and calculating the binding energies, followed by temperature, averaging the results using the Boltzmann factor and calculating the temperature-dependent interaction parameter. (ii) Off-lattice calculations are used, meaning that molecules are not arranged on a regular lattice as in the original Flory-Huggins theory. The coordination number is explicitly calculated for each of the possible molecular pairs using molecular simulations. These two extensions of the classical Flory-Huggins theory of mixing are documented in publications by Blanco [34] and Fan *et al.* [35].

3. Nanostructured polymer blends

The categories of nano-sized materials are quite challenging because of the intensive heterogeneity of their compositions and shapes. Different approaches can be used to classify carbon nanostructures; the suitable classification devise solely depends on the field of application of the nanostructures. One approach assumes as the basis of classification the characterization of the size of nanostructured carbons. One can also base a classification on an analysis of the dimensionalities of the structures, which in turn are connected with the dimensionality of quantum confinement and, thus, are related to nanoelectronic applications. Zero-dimension structures are fullerenes and diamond

clusters. One-dimensional structures are nanotubes. Two-dimensional structures are graphene, and three-dimensional structures are nanocrystalline diamond, and fullerite. Stone and Glass [36] reported a classification of carbon nanostructures (CNTs) based on the dimensional organization of their edge structures. Morphological benchmarks of the classification are provided, including a novel graphenated CNT hybrid which increases the linear edge density of nanostructured carbons by an order of magnitude.

The major challenging difficulty is to overcome the inherent immiscibility of polymers by using compatibilizing agents to allow for a sufficient mixing into nanoscopically sized domains of the dispersed phase. In industry, most commonly reactive blending or, similarly, the addition of block copolymers is used for compatibilizing the two components. One of the major drawbacks of this approach is that much of the block copolymer stabilizer does not adsorb at the interface and is lost during the high shear extrusion process, thus significantly increasing the cost of the polymer blend. A new method involves using Janus particles [37]. Janus particles are compartmentalized colloidal particles, which show segregation into two hemispheres. These particles uniquely combine the Pickering effect with amphiphilicity and are thus surfactant particles [38]. It has been calculated and experimentally shown for liquid-liquid interfaces that these particles adsorb strongly at interfaces, in particular stronger than standard surfactants or homogeneous particles. Figure 3 shows a classic

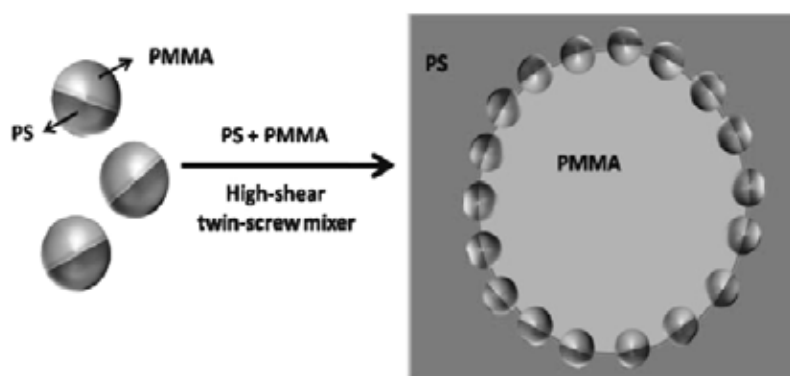


Figure 3. Schematic representation of Janus particles as compatibilizers and their adsorption at the blend interface of a PS/PMMA blend.

case where Janus particles are adsorbed at a blend interface. To simulate the effects of Janus nanoparticles and their effects on the miscibility of nanopolymer blends MD simulations are used. Molecular dynamics simulations help understand the translational and rotational diffusion of Janus nanoparticles at the interface between two immiscible nanopolymers. Self-assembly of nanoparticles at fluid interfaces has enabled the preparation of high quality two-dimensional crystals that can be employed for the fabrication of capsules, ultra-thin cross-linked membranes, and free-standing metal films. Figure 4 shows a typical simulation interface containing a spherical Janus particle at the interface with a specific orientation. Large-scale simulations can determine the best parameters of density,

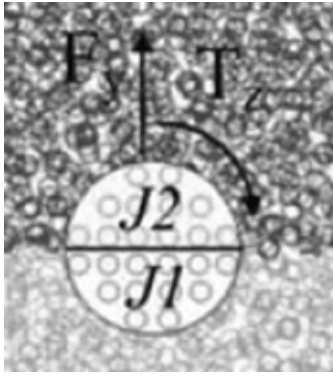


Figure 4. A spherical Janus particle at the interface between two immiscible nanopolymers at the start of large-scale molecular dynamics simulations.

diffusivity, Janus particle size and concentrations that can stabilize the interface and ensure miscibility.

4. Some design examples

Figure 5 shows a 3D printed thin artificial skin onto a biopaper using a bioink with fibroblast cells and several intermediate layers [39]. The biopaper is essentially a polymer blend design. But there are several improvements here that are sorely needed – including scaffolding that after healing is able to be biodegradable and replaceable by native cells that are constantly remodeling their internal structure and altering their mechanical properties. This will lead to the ultimate goal of organ design. By designing *via* simulations/computations it is possible to use the techniques of nanostructured polymer blend design methods to test various types of biopaper compatibilized with Janus particles.

Figure 6 shows the need for high-performance materials in low temperature, high radiation environments like low earth orbit where new materials are needed to create increased resistance of damage from growing space debris. Similarly the problem of atomic oxygen fluences due to the upper ozone layer on thousands of satellites is not overcome. Examination of Columbia space shuttle debris in the leading edge of the breached left wing indicated temperatures inside structural subsystems exceeded 1,760 °C which resulted in complex melt deposits on many components and failure like that shown in Figure 6. Current methods now enable the use of large-scale computations [40]. After a



Figure 5. 3D printed thin artificial skin.

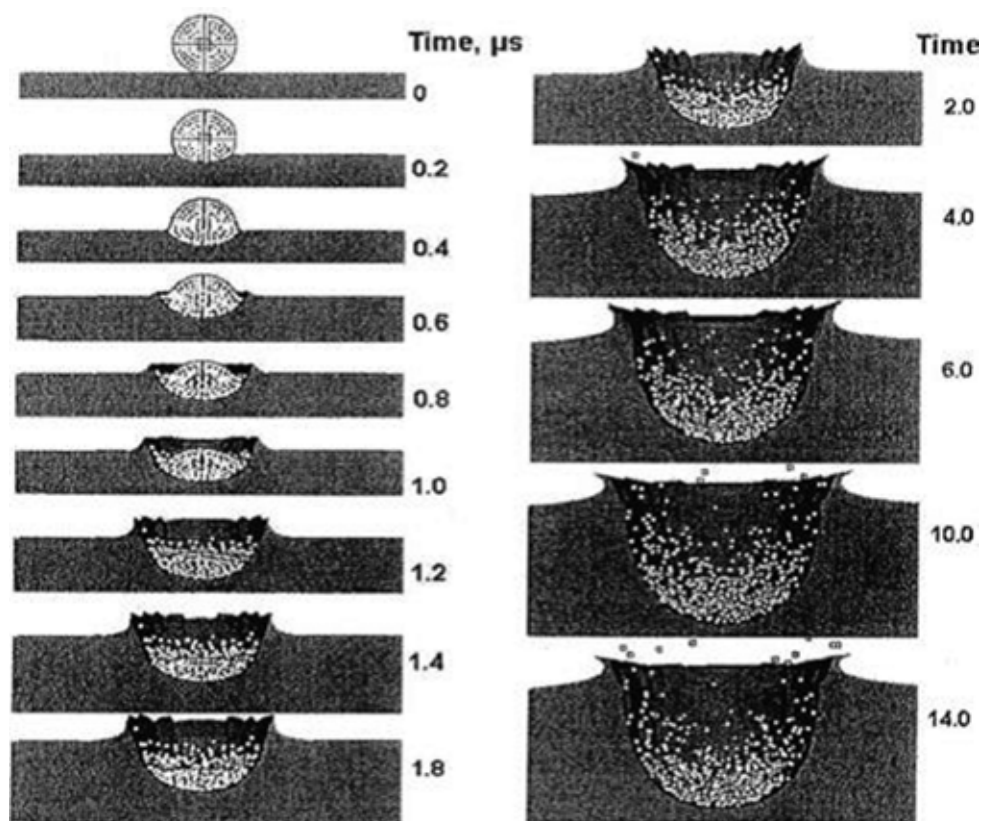


Figure 6. A simulation showing the hypervelocity impact of a micro-projectile in a polymeric material. For low orbit satellites to maintain optics and other functionality indefinitely there is a need for high impact resistance at the microscopic scale (due to space debris) at low temperature and a high radiation level tolerance without degradation. Polymer blend design creates new materials to solve this problem.

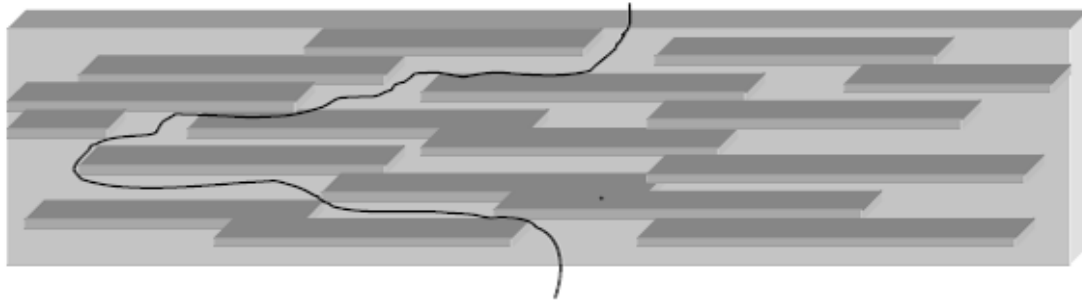
particular polymer blend or polymer nanocomposite is designed hypervelocity simulations for example are carried out to determine the impact on the polymeric material.

Figure 7 shows another example where nanoplatelets (a polymer blend with directional stability and a predefined set of mechanical properties) are dispersed in a substrate (also polymer based), but creates a barrier. So the permeability is controlled. This is the basis for artificial lungs [41] that can be used in extreme diving and artificial lung implants. Here again the use of polymer blend design methods facilitate the analysis of the stability and property predictions of the new materials on a thermodynamic scale.

Consider the case of developing supercapacitors for storage of energy - from a solar cell or for automatic rectification in high voltage electric grids [42]. In Figure 8 is the example of using say

a capacitor electrode coating “Backing X” - a nano-polymer blend reinforced by carbon nanotubes - that is predicted by simulations. However due to fabrication limitations we get an observed specific power that we want to improve when we make such a device. We redo the simulations including the modified fabrication parameters that built it. Note the device was never built; hence we had no prior data. Now with the new simulations we get an improved electrode coating (“Backing Y”) that we use and fabricate the device. And we have improved power and energy capacity. Without this there would be a plethora of random experimental options and the targeted approach would be lost.

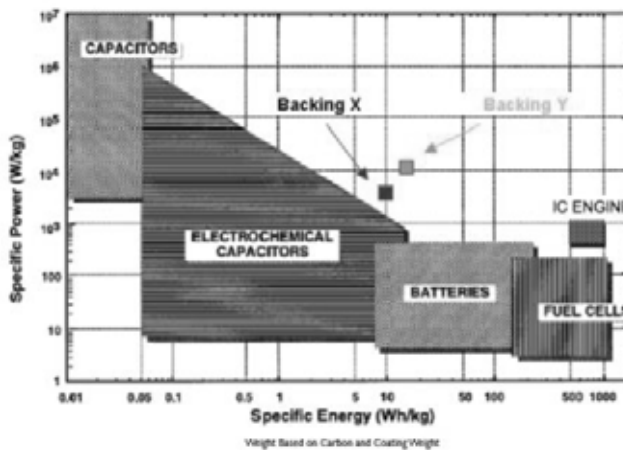
These are some of the many applications of computationally based polymer blend design for extreme environments. In areas of morphology control in dispersion and alignment, using these methods will enable the rapid development of new



Permeation path imposed by nanoplatelet modification of polymer films

Figure 7. Nanoplatelet modification of polymer films by polymer blend design.

Adding "Nano Sand" Increases Carbon Capacitance



Coating Increases Capacitance of Carbon Materials

Figure 8. "Backing X" v/s "Backing Y". The interplay of nano-polymer blend simulation with fabrication and testing. An example of targeted material design.

composites including nanolevel construction using carbon nanotube or exfoliated graphite (graphene) scaffolds with polymer blends. The scope of using this method is very wide – from new solar cells for extreme environments to ionomeric membranes for desalination and water purification.

Widely used polymers such as polystyrene and polyethylene are spectacularly boring in one sense: they repeat the same monomer over and over again. Their one-note tune is especially monotonous when compared with the quadruphonic symphony of DNA, which encodes an entire genome with 4 monomers; or the baroque masterpiece of a protein, drawing from 23 amino acids to build a complex 3D structure. Polymer blend design is now being

extended to sequence-controlled polymers [43]. One of the most challenging frontiers of polymer research is to tailor synthetic polymers with the same precision, so that chemists can fine-tune the electronic and physical properties of their products. Sequence-controlled polymers contain monomers in a predetermined order, forming strands of a very specific length. A dozen drugs approved by the US Food and Drug Administration use a polymer called polyethylene glycol to shield them from the body's immune system, improve their solubility or prolong their time in the body. Sequence-controlled polymers provide a more predictable biological effect, because every strand would be of the same length and shape, and its chemistry could be carefully



Figure 9. A flexible photovoltaic cell on a soap bubble, designed using large-scale polymer blend simulations.

designed to assist its drug cargo in the most useful way. This is again a limited set of uses of this design paradigm in the field of sequence-controlled polymers. Other uses of the field of sequence-controlled polymer design include storage of data in a more compact and inexpensive form than can conventional semiconductor technology (IARPA initiative [44]) in extreme operating environments. This is all made possible by large-scale computational modeling before any experimental testing.

Miniature flexible photovoltaics are difficult to design and make [45]. Their use in extreme environments will provide breakthroughs in robot and micro aerial vehicle design for high altitude and space applications. Using large-scale polymer blend simulations the design of a stable and flexible photovoltaic cell (Figure 9) for extreme environments is being done. Further at the nano-scale, self-assembly with controlled phase separation is also being studied *via* large-scale computational simulations.

5. Summary

There is a wide available literature that shows good agreement between the modeling and the experimental results. Simulations are a valuable tool in the prediction of the miscibility and phase behavior of polymer blends; particularly in cases where the polymers under consideration are not available. The research of polymer blends, or alloys, has experienced enormous growth in size and sophistication in terms of its scientific base,

technology and commercial development. As a consequence two very important issues arise: the increased availability of new materials and the need for materials with better performance. The advantages of polymer blends lie in the ability to combine existing polymers into new compositions thereby obtaining materials with specific properties. This strategy allows for savings in research and development of new materials with equivalent properties, as well as versatility, simplicity, relatively low cost and faster development time of new materials. As increased use of large chemical and polymer databases are coupled with the cheap availability of large-scale computing resources (both natively and in the cloud), mated with very fast network backplanes and high speed parallelized storage, it is now very easy to do large-scale polymer blend design simulations. Not only can one design such materials but also test them *via* large-scale modeling in the extreme environments they were designed to function in.

CONFLICT OF INTEREST STATEMENT

The author declares that there is no conflict of interest.

REFERENCES

1. Roy, N. K., Potter, W. D. and Landau, D. P. 2004, *Applied Intelligence*, 20(3), 215.
2. Roy, N. K., Potter, W. D. and Landau, D. P. 2006, *IEEE Transactions on Neural Networks*, 17(4), 1001.

3. Walsh, D. J. and Rostami, S. 1985, *Adv. Polym. Sci.*, 70, 119.
4. Young, R. J. and Lovell, P. A. 2011, *Multicomponent Polymer Systems. Introduction to Polymers*. 3rd ed., Boca Raton: CRC, 449-55.
5. Paul, D. R. and Newman, S. (Ed.) 1978, *Polymer Blends*: Academic Press: New York, Vols.1, 2.
6. Landry, C. J. T, Massa, D. J., Teegarden, D. M., Landry, M. R., Henrichs, P. M., Colby, R. H. and Long, T. E. 1993, *Macromolecules*, 26, 6299.
7. Fluegel, A. 2007, *Glass Technol.: Europ. J. Glass Sci. Technol. A*, 48(1), 13.
8. Olabisi, O., Robeson, L.M. and Shaw, M.T. 1979, *Polymer-Polymer Miscibility*, Academic, New York, Chap.3.
9. Rodgers, P. A. J. 1993, *Appl. Polym. Sci.*, 48, 1061.
10. Sanchez, I. C. and Lacombe, R. H. 1976, *J. Phys. Chem.*, 80, 2352.
11. Sanchez, I. C. and Lacombe, R. H. 1978, *Macromolecules*, 11, 1145.
12. Flory, P. J. 1953, *Principles of Polymer Chemistry*, Cornell University Press: Ithaca, NY.
13. White, R. P. and Lipson, J. E. G. 2009, *J. Chem. Phys.*, 131, 074110.
14. Ferry, J. D. 1980, *Viscoelastic Properties of Polymers*, 3rd ed., Wiley, New York.
15. Roland, C. M. and Ngai, K. L. 1991, *Macromolecules*, 24, 2261.
16. Doxastakis, M., Kitsiou, M., Fytas, G., Theodorou, D. N., Hadjichristis, N., Meier, G. and Frick, B. 2000, *J. Chem. Phys.*, 112, 8687.
17. Lutz, T. R., He, Y., Ediger, M. D., Cao, H., Lin, G. and Jones, A. A. 2003, *Macromolecules*, 36, 1724.
18. Haley, J. C. and Lodge, T. P. 2004, *Colloid Polym. Sci.*, 282, 793.
19. He, Y., Lutz, T. R. and Ediger, M. D. 2003, *J. Chem. Phys.*, 119, 9956.
20. Chung, G. C., Kornfield, J. A. and Smith, S. D. 1994, *Macromolecules*, 27, 964.
21. Ngai, K. L. and Roland, C. M. 2004, *Rubber Chem. Technol.*, 77, 579.
22. Luettmer-Strathmann, J. 2005, *J. Chem. Phys.*, 123, 014910.
23. Grosberg, A. Y. and Khokhlov, A. R. 1994, *Statistical Physics of Macromolecules*, AIP Series in Polymers and Complex Materials American Institute of Physics, Woodbury, NY.
24. Graessley, W. W. and Edwards, S. F. 1981, *Polymer*, 22, 1329.
25. Fetters, L. J., Lohse, D. J., Milner, S. T. and Graessley, W. W. 1999, *Macromolecules*, 32, 6847.
26. León, S., van der Vegt, N., Delle Site, L. and Kremer, K. 2005, *Macromolecules*, 38, 8078.
27. Neelakantan, A., May, A. and Maranas, J. K. 2005, *Macromolecules*, 38, 6598.
28. Kamath, S., Colby, R. H. and Kumar, S. K. 2003, *Macromolecules*, 36, 8567.
29. Faller, R. 2004, *Macromolecules*, 37, 1095.
30. Pan, X. and Shaffer, J. S. 1996, *Macromolecules*, 29, 4453.
31. Wang, Y., Ren, J. W., Zhang, C. Y. and He, M. C. 2016, *RSC Advances*, 6(103), 101323.
32. Mayo, S. L., Olafson, B. D. and Goddard, W. A. 1990, *Journal of Physical Chemistry*, 94, 8897.
33. Schweizer, K. S. and Curro, J. G. 1989, *J. Chem. Phys.*, 91, 5059.
34. Blanco, M. 1991, *Journal of Computational Chemistry*, 12(2), 237.
35. Fan, C. F., Olafson, B. D. and Blanco, M. 1992, *Macromolecules*, 25, 3667.
36. Stone, B. R. and Glass, J. T. 2012, *Diam. Relat. Mater.*, 23, 130.
37. Binks, B. P. and Fletcher, P. D. I. 2001, *Langmuir*, 17, 4708.
38. Walther, A. and Muller, A. H. E. 2008, *Soft Matter*, 4, 663.
39. Nakamura, M., Iwanaga, S., Henmi, C. and Arai, K. 2010, *Biofabrication*, 2, 1.
40. Frenkel, D. and Smit, B. 2001, *Understanding Molecular Simulation: From Algorithms to Applications* Academic Press, London.
41. Potkay, J. A. 2009, A high efficiency micromachine artificial lung, The 15th International Conference on Solid-State Sensors, Actuators and Microsystems (Transducers 2009), 2234.
42. Yang, X., Zhang, F., Zhang, L., Zhang, T., Huang, Y. and Chen, Y. 2013, *Adv. Funct. Mater.*, 23, 3353.
43. Lutz, J. F. 2010, *Polym. Chem.*, 1, 55.
44. <https://www.iarpa.gov/index.php/newsroom/iarpa-in-the-news/2016/828-the-plastics-revolution-how-chemists-are-pushing-polymer-s-to-new-limits>
45. Li, C., Liu, M. Y., Pschirer, N. G., Baumgarten, M. and Mullen, K. 2010, *Chem. Rev.*, 110, 6817.